ORIGINAL RESEARCH

Traumatic Brain Injury Disrupts Cerebrovascular Tone Through Endothelial Inducible Nitric Oxide Synthase Expression and Nitric Oxide Gain of Function

Nuria Villalba, PhD; Swapnil K. Sonkusare, PhD; Thomas A. Longden, PhD; Tram L. Tran, BSc; Adrian M. Sackheim, BSc; Mark T. Nelson, PhD; George C. Wellman, PhD; Kalev Freeman, MD, PhD

***Background*—**Traumatic brain injury (TBI) has been reported to increase the concentration of nitric oxide (NO) in the brain and can lead to loss of cerebrovascular tone; however, the sources, amounts, and consequences of excess NO on the cerebral vasculature are unknown. Our objective was to elucidate the mechanism of decreased cerebral artery tone after TBI.

***Methods and Results*—**Cerebral arteries were isolated from rats 24 hours after moderate fluid-percussion TBI. Pressure-induced increases in vasoconstriction (myogenic tone) and smooth muscle Ca^{2+} were severely blunted in cerebral arteries after TBI. However, myogenic tone and smooth muscle Ca^{2+} were restored by inhibition of NO synthesis or endothelium removal, suggesting that TBI increased endothelial NO levels. Live native cell NO, indexed by 4,5-diaminofluorescein (DAF-2 DA) fluorescence, was increased in endothelium and smooth muscle of cerebral arteries after TBI. Clamped concentrations of 20 to 30 nmol/L NO were required to simulate the loss of myogenic tone and increased (DAF-2T) fluorescence observed following TBI. In comparison, basal NO in control arteries was estimated as 0.4 nmol/L. Consistent with TBI causing enhanced NO-mediated vasodilation, inhibitors of guanylyl cyclase, protein kinase G, and large-conductance Ca^{2+}-activated potassium (BK) channel restored function of arteries from animals with TBI. Expression of the inducible isoform of NO synthase was upregulated in cerebral arteries isolated from animals with TBI, and the inducible isoform of NO synthase inhibitor 1400W restored myogenic responses following TBI.

***Conclusions*—**The mechanism of profound cerebral artery vasodilation after TBI is a gain of function in vascular NO production by 60-fold over controls, resulting from upregulation of the inducible isoform of NO synthase in the endothelium. **(*J Am Heart Assoc*. 2014;3:e001474 doi: 10.1161/JAHA.114.001474)**

Key Words: cerebral artery • endothelium-derived factors • myogenic tone • nitric oxide • traumatic brain injury • vascular endothelial function • vascular reactivity

Visits to emergency departments in the United States for traumatic brain injury (TBI) increased by nearly 30% between 2006 and 2010.[1] Despite the increasing public health concern, few options exist for medical management of brain trauma, and the fundamental basis of altered brain function during recovery from an injury are not understood. Concussive brain injuries can impair cerebral autoregulation[2–4] and decrease regional[5–7] and global[8] cerebral blood flow (CBF). Cerebral autoregulation, an essential function of the vasculature, serves to maintain constant flow over a range of blood pressures through myogenic, metabolic, and neurogenic mechanisms.[9] The myogenic component (*myogenic tone*) represents the intrinsic ability of smooth muscle (SM) to either constrict in response to increased intravascular pressure or to dilate when intravascular pressure drops. This autoregulatory mechanism normally provides protection against hypotension (and hypertension) by maintaining blood flow to the brain at relatively constant levels over a range of physiological blood pressures. However, impaired cerebral autoregulation occurs in the days following a TBI such that mild decreases in blood pressure can lead to cerebral hypoperfusion and ischemia.[5,7]

From the Departments of Pharmacology (N.V., S.K.S., T.A.L., M.T.N., G.C.W., K.F.) and Surgery (A.M.S., T.L.T., K.F.), University of Vermont, Burlington, VT, USA; Institute of Cardiovascular Sciences, University of Manchester, UK (M.T.N.).

An accompanying Video S1 is available at http://jaha.ahajournals.org/content/3/6/e001474/suppl/DC1

Correspondence to: Kalev Freeman, University of Vermont, Given E301, Burlington, VT, USA, 05405. E-mail Kalev.Freeman@uvm.edu

Received October 9, 2014; accepted November 13, 2014.

The role of nitric oxide (NO) in TBI-induced dysregulation of CBF is unclear and controversial. In healthy brains, NO acts as both a vasodilator and neurotransmitter, with production catalyzed by the Ca^{2+}/calmodulin-dependent NO synthase isozymes eNOS (NOS3) and neuronal isoform of NOS (nNOS; NOS1) in the vascular endothelium and nitrergic nerves, respectively.[10] Subnanomolar concentrations of NO induce significant vasodilation of small vessels,[11] and production of NO via eNOS in the endothelium plays a prominent role in the regulation of cerebral artery diameter and the autoregulatory response.[12] A third NOS isozyme, inducible isoform of NOS (iNOS; NOS2), is Ca^{2+} independent, constitutively active, and upregulated at the transcriptional level by proinflammatory cytokines.[13] iNOS is not normally expressed in brain tissue, but it may become pathologically upregulated by damage or injury, including TBI.[14–17]

Both excess and deficiency of NO, at different time points, can contribute to secondary injury after brain trauma.[18] Evidence of TBI-induced disruption of the microvascular endothelium[19] and diminished endothelial-dependent cerebral artery dilation[20,21] suggests that endothelial NO production may be impaired. Furthermore, a study indicating that inhaled NO improved CBF and reduced brain damage in a TBI model might suggest an endothelial NO deficiency, but vascular NO was not measured.[22] Conversely, reduced myogenic tone in cerebral arteries after a TBI[2,4,23] and improvement in tone with addition of a peroxynitrite scavenger[4] suggest that vascular NO may be increased, thereby disrupting autoregulation. Other reports indicate that neuronal NO is also increased after trauma because of cytokine-stimulated iNOS expression,[24] which leads to neuronal NO production.[14,15,25,26] Large increases in neuronal NO resulting from iNOS upregulation are cytotoxic and contribute to neuronal injury and death.[27] Selective inhibition of iNOS improves outcome in several experimental models of brain injury, including TBI.[28–30] The gap in knowledge about the sources and consequences of vascular NO after brain trauma is a critical barrier to the development of therapeutics such as iNOS inhibitors for medical management during recovery from brain injury.

In this study, our goal was to elucidate the source, quantity, and impact of altered NO signaling in cerebral arteries following a TBI, using a novel combination of approaches that included measurements of arterial diameter, SM Ca^{2+}, and live-cell imaging of 4,5-diaminofluorescein diacetate (DAF-2 DA) fluorescence under clamped NO conditions to index NO levels. We demonstrated that TBI causes a 60-fold increase in cerebral artery NO levels, severely blunting pressure-induced increases in SM Ca^{2+} and myogenic tone. Furthermore, we found that TBI-induced increases in cerebral artery NO are endothelial dependent and are driven by upregulation of iNOS in the endothelium.

Materials and Methods

TBI Model

Adult male Sprague-Dawley rats (aged 3 to 4 months; 300–350 g; Charles River, Saint Constant, Quebec, Canada) were used for these studies. Experimental animals were placed under anesthesia for a fluid-percussion injury to the left cerebral hemisphere, delivered through a craniotomy providing a highly reproducible, survivable brain injury with measurable neurological deficits.[31–33] Briefly, rats were anesthetized with 2% to 5% isoflurane. Craniotomy was performed at the midline between bregma and lambda (3 mm in diameter), and a 2-mm internal-diameter stainless-steel hollow intracranial screw was placed in the skull. Once secured, the intracranial screw was filled with 0.9% normal saline and attached by pressure tubing to a cylindrical reservoir filled with sterile isotonic saline. Injury was induced by releasing a pendulum that strikes the fluid column within the reservoir, causing a pressure wave that was transmitted through the tubing and cranial screw to the dural surface of the brain. Animals were allowed to recover with free access to food and water. Recovery was defined as the ability to maintain an upright posture, to ambulate, and to take oral hydration. Control animals were identical rodents without brain injury. All animals received buprenorphine analgesia (subcutaneous; 0.05 mg/kg) while under anesthesia and at 6 to 12 hours after surgery. Animals were euthanized at 24 hours post-injury by decapitation under deep pentobarbital anesthesia (intraperitoneal; 0.03 mg/kg) for harvesting of blood vessels for experiments. All studies were conducted in accordance with the NIH Guidelines for the Care and Use of Laboratory Animals (eighth edition) and approved by the Institutional Animal Care and Use Committee of the University of Vermont. Chemicals were purchased from Sigma-Aldrich, except as specifically noted.

Preparation of Intact Cerebral Arteries

At 24 hours post-injury, animals were euthanized to harvest the posterior cerebral arteries. With TBI model animals, the posterior cerebral arteries used for experimental study were obtained from a region adjacent to but not within the area of mechanical injury in this model, as defined by magnetic resonance imaging in our previous study.[31] For some experiments, arteries from the contralateral side of the injury were also studied. Posterior cerebral arteries (≈250 μm maximal diameter) were dissected immediately and placed in ice cold (4°C) artificial cerebrospinal fluid (aCSF) containing (in mmol/L) 125 NaCl, 3 KCl, 18 $NaHCO_3$, 1.25 NaH_2PO_4, 1 $MgCl_2$, 2 $CaCl_2$, 5 glucose, aerated with 5% CO_2, 20% O_2, and 75% N_2. Artery segments

(~2 mm in length) were cannulated on glass resistance-matched micropipettes filled with aCSF and pressurized using an electronic pressure servo with a transducer in a vessel chamber (Living Systems Instrumentation) while superfused with warmed (37°C), gassed aCSF.[33,34] Bath pH was monitored and maintained at 7.30 to 7.35.[35]

Ex Vivo Arterial Diameter and SM Ca^{2+} Measurements

Lumen diameter was recorded continuously using a charge-coupled device camera and edge-detection software (IonOptix 6.0; IonOptix). Vessels were allowed to equilibrate for 30 minutes at low pressure (10 mm Hg) and then stimulated with 60 mmol/L KCl (K^+) to verify vessel viability. To determine myogenic tone, responses of vessels to stepwise increases in intravascular pressure were measured over a pressure range of 20 to 100 mm Hg (20 mm Hg pressure steps). At 100 mm Hg, vessels were incubated for 15 minutes with aCSF containing 0 mmol/L Ca^{2+} and the vasodilators diltiazem (100 μmol/L) and forskolin (1 μmol/L) to achieve maximal diameter, and then a pressure-diameter curve (passive curve) was performed. Vessels with pressure leaks or those not responding to 60 mmol/L K^+ were not studied. Effect of the NO donor (spermine NONOate; Cayman Chemical), NOS inhibitors, large-conductance Ca^{2+}-activated potassium channel (BK) inhibitor (paxilline, 1 μmol/L) and protein kinase G (PKG; $R_{(P)}$-8-Br-cGMPS, 1 μmol/L) were determined at an intraluminal pressure of 70 mm Hg. The following NOS inhibitors were used: Nω-nitro-L-arginine (L-NNA; 100 μmol/L); N-([3-(aminomethyl)phenyl]methyl)-ethanimidamide, dihydrochloride (1400W; 10 μmol/L); and N-([4S]-4-amino-5-[(2-aminoethyl)amino]pentyl)-N′-nitroguanidine tris(trifluoroacetate) (AAAN; 30 μmol/L; Santa Cruz Biotechnology). The 1400W compound was administered in the presence of its cofactor, NADPH (125 μmol/L). For some experiments, the endothelial layer was mechanically disrupted by repeated insertion of a human hair into the arterial lumen. The effectiveness of endothelium removal was confirmed by absence of responses to the endothelium-dependent vasodilator 6,7-dichloro-1H-indole-2,3-dione 3-oxime (NS309, 1 μmol/L).[36]

Percentage of myogenic tone at each pressure was calculated as the percentage decrease of the lumen (inner) and vessel (outer) diameters of arteries in Ca^{2+}-free aCSF from the following equation: tone (%)=[(DP−DA)/DP]×100. DP indicates the (passive) lumen diameter of the artery in Ca^{2+}-free aCSF containing the vasodilators diltiazem (100 μmol/L) and forskolin (1 μmol/L), and DA indicates the (active) lumen diameter of the artery in Ca^{2+}-containing aCSF. Similarly, other data were expressed as percentage of vasodilation, which was calculated as the difference in diameter before and after agonist administration normalized to the maximal diameter. Percent change in diameter (percentage of constriction, decrease in diameter) was calculated from baseline with the following equation: $(D_{drug}-D_{baseline}/D_{baseline})\times 100$. D_{drug} is the lumen diameter exposed to the given drug, and $D_{baseline}$ is the lumen diameter prior to adding the drug. Percentage of vasodilation to spermine NONOate was normalized to maximal dilation and calculated with the following equation: $([D_{spermine\ NONOate}-D_{start}]-[DP-D_{start}])\times 100$. $D_{spermine\ NONOate}$ is the lumen diameter at a specific concentration of spermine NONOate, D_{start} is the diameter prior to giving the first concentration of spermine NONOate, and DP is the lumen diameter of the artery in Ca^{2+}-free aCSF containing the vasodilators diltiazem (100 μmol/L) and forskolin (1 μmol/L).

Simultaneous Arterial Wall $[Ca^{2+}]_i$ and Diameter Measurements in Intact Cerebral Vessels

Vascular SM-specific loading with the ratiometric Ca^{2+} indicator dye Fura-2 AM (acetoxymethyl ester, membrane-permeant form; Invitrogen) allowed simultaneous monitoring of changes in vascular SM intracellular Ca^{2+} concentration ($[Ca^{2+}]_i$), as described previously.[33,34] After cannulation, specific loading of vascular SM cells was performed with the ratiometric Ca^{2+} indicator dye Fura-2 AM (10 μmol/L) and pluronic acid (0.05%; Invitrogen) in aerated aCSF at room temperature in the dark for 45 minutes. Afterward, Fura-2–loaded arteries were allowed 30 minutes for de-esterification of Fura-2 AM by continuous superfusion with aerated aCSF at 37°C. For ratiometric measurements of Fura-2 AM, the vessel chamber was placed on an inverted fluorescence microscope (Nikon TE2000-S) equipped with a photomultiplier system (IonOptix). Arteries were excited with alternating 340- and 380-nm wavelengths, and ratio images were obtained from background corrected images of the 510-nm emission using software developed by IonOptix.[34] In a separate set of experiments, R_{min}, R_{max}, and β were measured from arteries treated with ionomycin (10 μmol/L) and nigericin (5 μmol/L). R_{min} and R_{max} are the emission ratios under Ca^{2+}-free (5 mmol/L EGTA) and Ca^{2+}-saturated (10 mmol/L $CaCl_2$) conditions, respectively. β was determined as the ratio of F_{380} intensities at R_{min} and R_{max} (Table 1). An apparent dissociation constant (K_d) of 282 nmol/L of Fura-2 was used as previously calculated for cerebral arteries after in situ calibration.[33] Arterial wall $[Ca^{2+}]_i$ was estimated by using the equation described by Grynkiewicz et al:[37] $[Ca^{2+}]=K_d\times\beta\times(R-R_{min})/(R_{max}-R)$. Average values were significantly different between groups; therefore, individual values for each group of animals were used for $[Ca^{2+}]_i$ estimation (Table 1).

Table 1. Ratios of Emission Signals Under Ca^{2+}-Free and Ca^{2+}-Saturated Conditions (R_{min} and R_{max}, Respectively) and Ratio of F_{380} Intensities at R_{min} and R_{max} (β) Determined From a Separate Set of Arteries From Control and TBI Rats

	Control	TBI
R_{max}	4.62±0.64	6.24±1.52*
R_{min}	0.40±0.04	0.41±0.02
β	6.28±0.30	7.48±1.52*
n	5	4

Average values are significantly different between groups, so individual values shown for arteries from control and TBI animals were used for analysis of intracellular Ca^{2+} concentration measurements. TBI indicates traumatic brain injury. Wilcoxon rank-sum, *P<0.05.

Estimation of NO Concentration in Intact Cerebral Arteries

Fixed concentrations of NO were delivered to both pressurized and surgically opened cerebral arteries from control animals to determine the amount of NO required to replicate the decreased myogenic tone and increased 4,5-diaminofluorescein triazole (DAF-2T) fluorescence observed in arteries from TBI animals. NO solutions at controlled and constant concentrations were set using an NO-clamp approach developed by Griffiths.[19,38] This method provides stable, known NO concentrations using the combination of an NO donor and an NO scavenger. Spermine NONOate was selected as an NO donor because it has a long half-life (39 minutes) and releases a controlled amount of NO in solution; a cell-permeable NO scavenger, carboxy-2-phenyl-4,4,5,5-tetramethylimidazoline-1-oxyl-3-oxide (CPTIO; Enzo Life Sciences), was elected as a source of NO consumption. L-NNA was added to the experiments to inhibit endogenous NO production. Using a mathematical model (K. Held, PhD, W. Dostmann, PhD, personal communication, 2014), we resolved the series of differential pharmacokinetic equations with computer software (MathCad 1.0; Parametric Technology Corporation) to determine the concentrations of NO donor and NO scavenger needed to clamp the NO concentration at a constant level in the presence of L-NNA to inhibit endogenous NO production. The concentrations of spermine NONOate, CPTIO, and L-NNA we used to generate clamped NO solutions, delivered in an increasing stepwise fashion from 0.1 to 30.0 nmol/L, are provided in Table 2.

Live Native Cell Imaging of DAF-2T Fluorescence to Index NO Levels

The nonfluorescent compound DAF-2 DA reacts with NO to yield highly fluorescent DAF-2T.[39] For live native endothelial cell imaging, arteries were surgically opened and pinned down

Table 2. Nitric Oxide Clamp With the Individual Determined Concentrations of NO Donor and NO Scavenger (CPTIO)

	Spermine NONOate	
Clamped [NO]	NO Donor	CPTIO
1 nmol/L	2 μmol/L	60 μmol/L
2 nmol/L	4 μmol/L	60 μmol/L
3 nmol/L	5 μmol/L	60 μmol/L
4 nmol/L	6 μmol/L	50 μmol/L
5 nmol/L	8 μmol/L	60 μmol/L
6 nmol/L	10 μmol/L	60 μmol/L
7 nmol/L	10 μmol/L	50 μmol/L
10 nmol/L	15 μmol/L	50 μmol/L
20 nmol/L	75 μmol/L	60 μmol/L
30 nmol/L	100 μmol/L	60 μmol/L

Table showing desired NO concentrations from 1 to 30 nmol/L provided by the combination of spermine NONOate and CPTIO. CPTIO indicates carboxy-2-phenyl-4,4,5,5-tetramethylimidazoline-1-oxyl-3-oxide; NO, nitric oxide.

on a Sylgard-coated dish with the endothelial surface up (*en face* preparation). Arteries were loaded in the dark with DAF-2 DA (10 μmol/L) in the presence of pluronic acid (0.05%) dissolved in aerated physiological saline solution of the following composition (in mmol/L) for an hour at 32°C: 118.5 NaCl, 4.7 KCl, 24 $NaHCO_3$, 1.18 KH_2PO_4, 2.5 $CaCl_2$, 1.2 $MgCl_2$, 0.023 EDTA, and 11 glucose (pH 7.4). NO levels were indexed in both vascular endothelium and SM cells under flow conditions and at 37°C; images were acquired at 30 to 35 images per second by using an Andor Technology Nipkow spinning-disc confocal system coupled to a Nikon Eclipse E600 FN upright microscope with a 60× water-dipping objective (numerical aperture 1.0) and an electron-multiplying charge-coupled device camera, as we have described previously.[40] Fluorescence was detected using an excitation wavelength of 488 nm, and emitted fluorescence was collected using a 527- to 549-nm band-pass filter; the same laser intensity was used for all experiments. DAF-2T fluorescence was measured offline in the collected image by an average fluorescence of 10 images from the same field, using custom-designed software (A. Bonev, University of Vermont, Burlington, VT).[41] The area of each endothelial cell or vascular SM surface was determined by drawing a freehand region of interest (ROI) around the outline of the individual cells. Global DAF-2T fluorescence was measured over the entire area of a cell and averaged by the number of cells per field. In some experiments, slit-open arteries were incubated for 1 hour at 32°C with L-NNA (300 μmol/L) and/or CPTIO (60 μmol/L) prior to loading of the DAF-2 DA to inhibit endogenous NO production or scavenger NO, respectively. The L-NNA and/or CPTIO concentrations were maintained during loading and

imaging. DAF-2T fluorescence was normalized to basal levels obtained from control arteries in the endothelium or SM. Video images were acquired from either endothelium or vascular SM for 2 minutes. For quantification of NO levels in live endothelial or SM cells, confocal fields containing >12 cells in cross-section were selected for imaging, and images were obtained for that field for the 2-minute period. Images at the same time point (30 seconds) after starting image acquisition were analyzed offline.

Clamped Nitric Oxide Experiments on Pressurized Cerebral Arteries

Arteries were cannulated and pressurized to 80 mm Hg, as described above. Basal NO was then decreased to 0 nmol/L clamped condition by adding 60 μmol/L CPTIO plus 100 μmol/L L-NNA and superfusing for 20 minutes. After that, cumulative concentrations of spermine NONOate were added to the solution in the presence of CPTIO and L-NNA, increasing in a stepwise fashion from 0.1 to 30 nmol/L (Table 2).

mRNA Expression of NOS Isozymes

Total RNA was obtained from cerebral arteries of control and TBI animals using a Trizol isolation procedure and reverse transcribed into cDNA with the High Capacity cDNA Kit (Applied Biosystems). Quantitative polymerase chain reaction (qPCR) was performed using an ABI PRISM 7900HT Sequence Detection System (Applied Biosystems); iNOS-, eNOS-, nNOS-, and GAPDH-specific primers; and PerfecCta qPCR supermix (Quanta Biosciences), as reported previously.[42] Briefly, a total of 6.6 ng of DNAse I-treated RNA was reverse transcribed into cDNA using the High Capacity cDNA Kit (Applied Biosystems) in a 20 μL reaction. Moreover, qPCR was performed in duplicate for each sample using 1 μL of cDNA as a template for all NOS targets, 1× PerfeCta qPCR supermix (Quanta Biosciences), and 1× Taqman gene expression assays in a 20 μL reaction. qPCR was carried out in an ABI PRISM 7900HT Sequence Detection System (Applied Biosystems) using the following conditions: 45°C for 5 minutes and 95°C for 3 minutes followed by 40 cycles of 15 seconds at 95°C and 45 seconds at 60°C. We amplified GAPDH as a normalizing internal control. To calculate the relative index of gene expression, we used the $2^{-\Delta\Delta Ct}$ method[43] using control samples for calibration.

Drugs, Chemical Reagents, and Other Materials

The NO donor solutions were prepared freshly before the experiments in 10 mmol/L NaOH and kept in ice; each aliquot of the solutions was used for only 24 hours. CPTIO was prepared in DMSO as 50 mmol/L stock, and then aliquots were frozen.

Statistical Analysis

Values are presented as mean±SEM. For clamped NO experiments, concentration-response curves were calculated with GraphPad Prism software (version 6.03; GraphPad Software, Inc) to fit the Hill slope from the data (variable slope model) for each individual experiment and then averaged to obtain the mean and SEM values. Statistical comparisons were performed using GraphPad Prism. Because of generally small sample sizes, the nonparametric tests (Wilcoxon rank-sum) were used for comparison between 2 groups. We also used repeated measures analysis of variance (ANOVA) for the comparison of multiple groups at different concentrations. Statistical significance was considered at the level of $P<0.05$.

Results

Myogenic Tone and Pressure-Dependent Increases in Smooth Muscle Ca^{2+} Are Abolished After TBI

To determine the impact of TBI on the cerebral vasculature, simultaneous measurements of SM Ca^{2+} and lumen diameter were made using isolated pressurized posterior cerebral arteries obtained from brains of control and TBI animals (Figure 1). At low intravascular pressure (20 mm Hg), SM Ca^{2+} concentrations were 144±20 nmol/L and 105±18 nmol/L in cerebral arteries from control and TBI animals, respectively. In response to stepwise increases in intravascular pressure, arteries from control animals showed the expected increase in SM Ca^{2+} and vasoconstriction (ie, developed myogenic tone).[33] At 60 mm Hg, for example, SM Ca^{2+} was increased to 383±16 nmol/L (n=5), whereas arterial constriction was reduced to 27±8% (n=5) of maximally dilated diameter. In contrast, pressure-dependent increases in SM Ca^{2+} and vasoconstriction were severely blunted in ipsilateral (injury side) arteries from TBI animals; the difference between groups was particularly pronounced at physiological pressures between 60 and 100 mm Hg. At 60 mm Hg, pressure-induced constrictions were absent, and SM Ca^{2+} (159±27 nmol/L, n=6) was minimally increased in arteries isolated from TBI animals (Figure 1C and 1D). Both the thromboxane A_2 analog, U46619 (100 nmol/L), and elevation of external K^+ to 60 mmol/L also constricted ipsilateral arteries from TBI animals to a lesser extent than controls (Figure 2A and 2B). Cerebral artery impairment was not limited to the ipsilateral side of the brain injury; arteries isolated from the

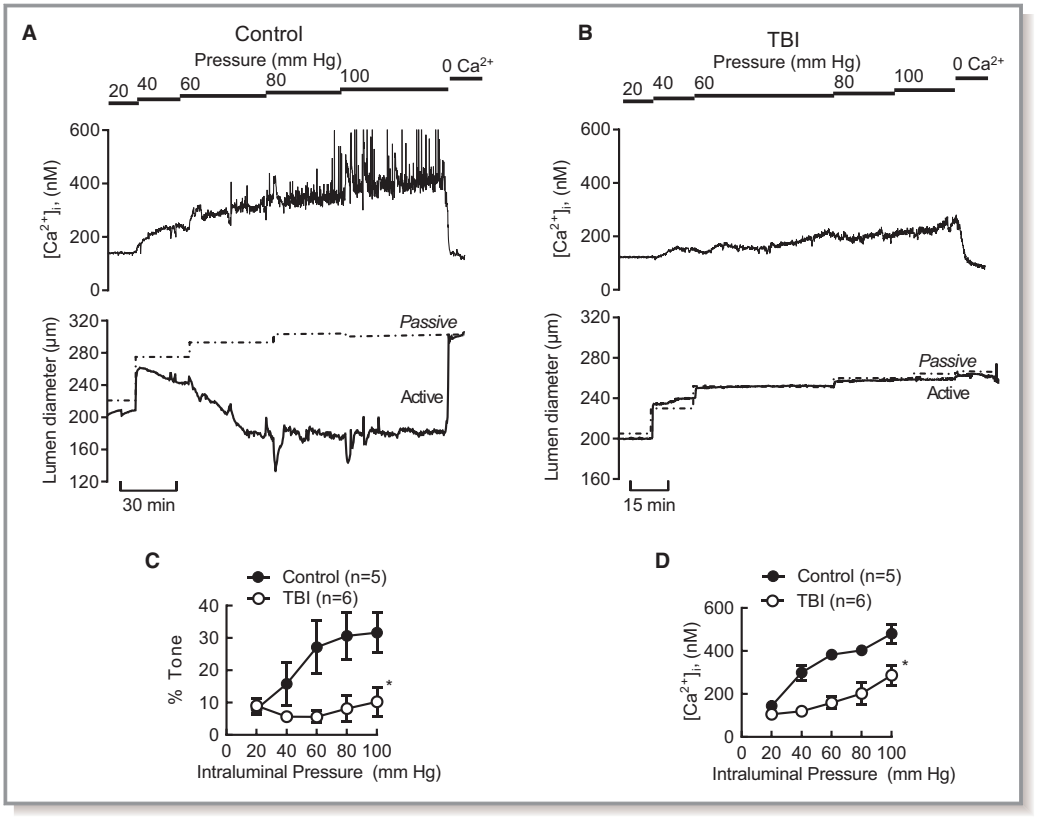

Figure 1. Decreased cytosolic Ca^{2+} and myogenic tone in cerebral arteries from TBI animals. A and B, Representative traces showing simultaneous $[Ca^{2+}]_i$ and lumen diameter measurements obtained from intact cerebral arteries isolated from control (A) and TBI (B) animals. Recordings were obtained during stepwise increases in intravascular pressure (20 to 100 mm Hg). C and D, Summary of myogenic tone (C) and $[Ca^{2+}]_i$ (D) obtained from control (n=5) and TBI (n=6) animals. *P<0.05, repeated measures one-way ANOVA. $[Ca^{2+}]_i$ indicates intracellular Ca^{2+} concentration; TBI indicates traumatic brain injury.

contralateral side of TBI animals showed a similar reduction in pressure-induced constrictions (Figure 3). Despite the marked depression of the ability of arteries from TBI animals to constrict to vasoactive stimuli, the fully dilated diameters of arteries from control and TBI animals that were relaxed by Ca^{2+}-free aCSF containing the vasodilators diltiazem (100 µmol/L) and forskolin (1 µmol/L) were not significantly different (Figure 4).

These data demonstrate a dramatic reduction in cerebral arterial tone following TBI that is diffuse and that is not limited to arteries near the site of injury. This impaired myogenic response persists despite removal of the arteries from the animal and could reflect enhanced vasodilatory signals emanating from cerebral arteries after TBI.

NO Is Elevated in Cerebral Arteries Following TBI

Nitric oxide, a potent dilator of the systemic[44] and cerebral vasculature,[9] is increased in the brain after TBI in a variety of species, including humans.[14] To examine whether the concentration of vascular NO, specifically, is increased in cerebral arteries isolated after TBI, confocal imaging was performed using surgically opened cerebral arteries loaded with the NO indicator DAF-2 DA[15] (Figure 5). After TBI, fluorescence was increased 1.3-fold in live endothelial cells and 2.2-fold in SM cells compared with fluorescence in comparable tissue from control animals (Figure 5C and 5D). The possibility of NO diffusion between endothelium and SM limits our ability to designate the source of NO production. In addition, NOS inhibition with L-NNA (300 µmol/L) decreased DAF-2T fluorescence in both endothelium and SM from TBI animals to levels observed in control animals. These results demonstrate a marked elevation of NO in cerebral arteries following TBI.

Inhibition of NOS or Endothelial Removal Restores Cerebral Artery Function After TBI

To further explore TBI-induced increases in cerebral artery NO and its impact on vascular function, the effects of intravascular pressure on SM Ca^{2+} and diameter were examined in the presence of the broad-spectrum NOS

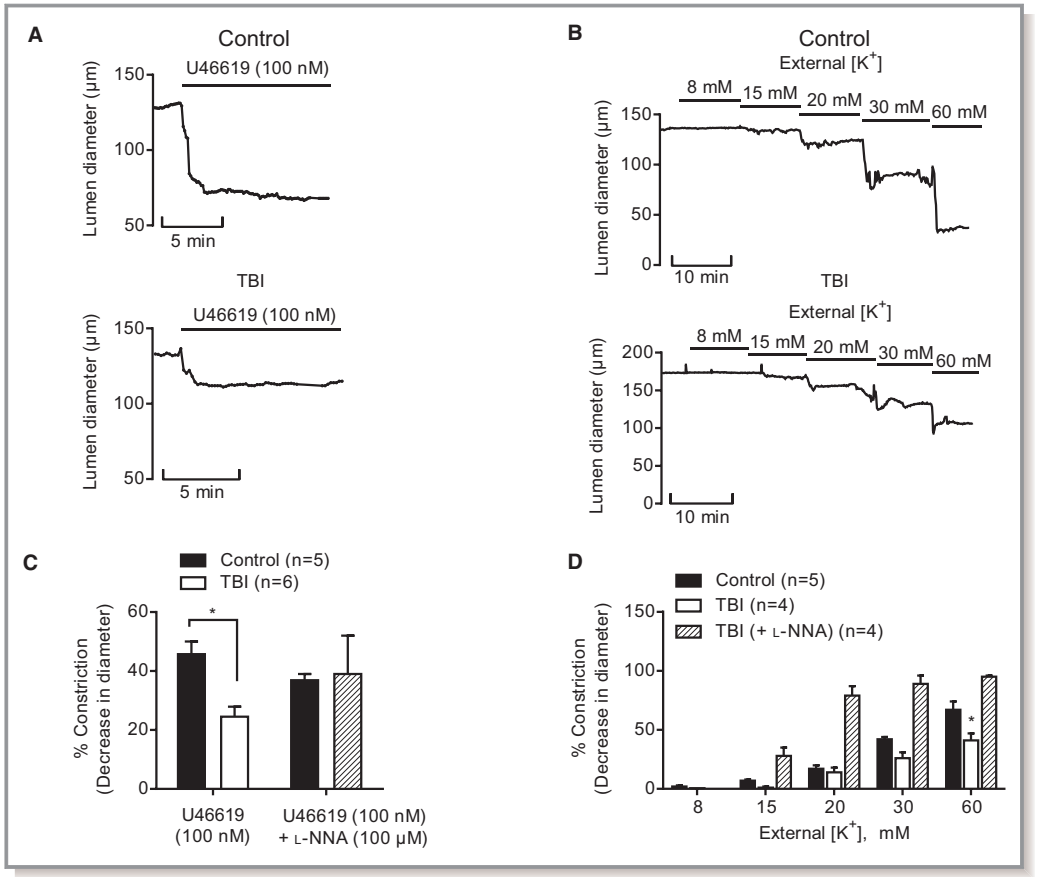

Figure 2. Effects of the thromboxane A_2 analog, U46619 and increased abluminal K^+ on the diameter of cerebral arteries. Representative traces showing vasoconstriction to (A) U46619 (100 nmol/L) and external K^+ (B) in control (upper) and TBI (bottom) cerebral arteries pressurized to 20 mm Hg. C and D, Summary data obtain from control (n=5) and TBI animals (n=4 to 6) in control conditions and after L-NNA (100 μmol/L) treatment. Wilcoxon rank-sum, **P*<0.05 Control vs TBI (U46619 responses); repeated measures one-way ANOVA, **P*<0.05 Control vs TBI (K^+ curve). L-NNA indicates Nω-nitro-L-arginine; TBI, traumatic brain injury.

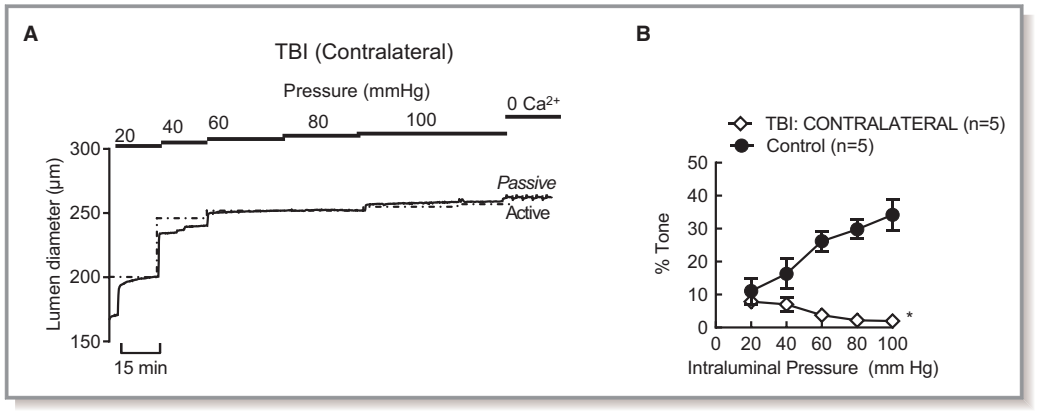

Figure 3. Vasoconstriction in response to pressure following TBI in cerebral arteries isolated from the contralateral side of the injury. A, Representative trace showing lumen diameter measurements obtained from intact cerebral arteries contralateral to the injury site from a TBI animal. Recordings were obtained during stepwise increases in intravascular pressure (20 to 100 mm Hg). B, Summary of percentage of myogenic tone obtained from control (n=5) and TBI (n=5) animals. **P*<0.05, repeated measures one-way ANOVA. L-NNA indicates Nω-nitro-L-arginine; TBI, traumatic brain injury.

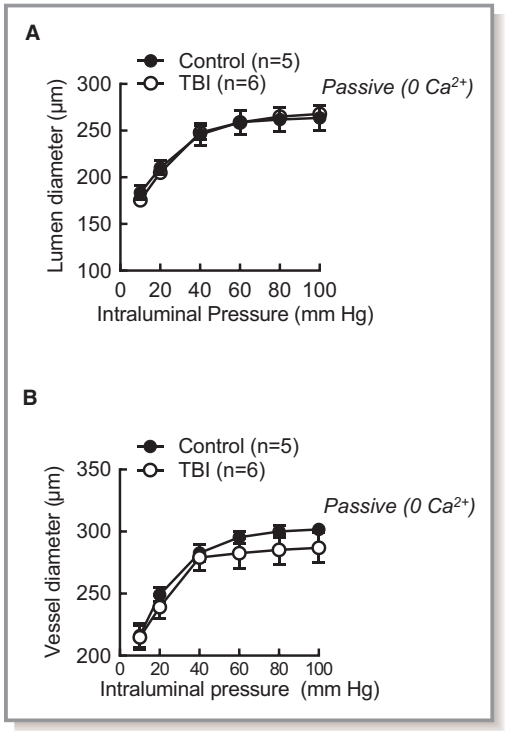

Figure 4. Passive physical properties between isolated cerebral arteries from control and TBI animals. Summary of passive lumen diameter (A) and vessel diameter (B) measurements of isolated cerebral artery segments at intravascular pressures from 10 to 100 mm Hg in Ca^{2+}-free artificial cerebrospinal fluid in the presence of forskolin and diltiazem. TBI indicates traumatic brain injury.

inhibitor L-NNA (100 µmol/L) (Figure 6A). Blockade of NO synthesis with L-NNA increased myogenic tone and SM Ca^{2+} in both control and TBI arteries, but the effect of L-NNA was greater in the TBI arteries, eliminating the differences between groups (compared with Figure 1). At 60 mm Hg, for example, in the presence of L-NNA, the SM Ca^{2+} (control: 348±27 nmol/L, n=4; TBI: 268±43 nmol/L, n=5) and myogenic tone (control: 28±4% constriction, n=4; TBI: 22±2% constriction, n=5) were similar in the 2 groups. Furthermore, constrictions to U46619 and elevated external K^+ were restored by L-NNA (100 µmol/L) in arteries from TBI animals (Figure 2C and 2D). To determine whether endothelial removal mimicked the effect of L-NNA, the lumen of some TBI arteries was mechanically disrupted before cannulation. As with L-NNA, myogenic tone in response to stepwise increases in intraluminal pressure was restored to control levels in endothelial-denuded arteries from TBI animals (Figure 6B through 6D). Denuding the arteries from TBI animals of endothelium eliminated the difference between groups. The myogenic response of intact arteries from control animals was not different from that of the arteries from TBI animals without endothelium (myogenic tone, control: 38±9%, n=5, TBI: 33±8%, n=5) (Figure 6B through 6D). These results indicate that the vascular endothelium serves as the source of excess NO leading to decreased cerebral artery constriction after TBI.

iNOS Upregulation in Cerebral Arteries Following TBI

The data presented indicate that TBI leads to a gain of function of endothelial NO production to cause a profound loss of pressure-induced vasoconstriction. To determine the NOS isoenzymes that contribute to increased NO following TBI, expression of eNOS, iNOS, and nNOS was assessed by qPCR (Figure 7A). iNOS was significantly increased (≈10-fold) in cerebral arteries from TBI animals compared with control animals. Interestingly, eNOS was unchanged, and nNOS was modestly but significantly decreased in arteries after TBI. To examine the functional impact of TBI-induced iNOS upregulation, pressurized arteries were exposed to the selective iNOS inhibitor 1400W.[45–47] Nonselective NOS inhibition with L-NNA caused constrictions in control arteries (15±2% n=5) but caused substantially greater constrictions in TBI arteries (32±4%, n=5; $P<0.05$) (Figure 7B and 7C). Inhibition of iNOS caused only a slight constriction in cerebral arteries from control animals; in contrast, cerebral arteries from TBI animals exhibited a marked constriction in response to iNOS inhibition (26±3%, n=4) (Figure 7B and 7D). The specific nNOS inhibitor AAAN[48] (30 µmol/L) did not alter tone in arteries from either control or TBI animals (Figure 7B). Furthermore, arteries from control and TBI animals responded similarly to an NO donor in the presence of L-NNA (100 µmol/L) (Figure 8A), demonstrating that NO sensitivity of vascular SM was unaltered by TBI. These data support the idea that, although basal eNOS-catalyzed NO production contributes to diameter regulation in arteries from control animals, endothelial iNOS upregulation underlies the NO gain of function and profound vasodilation observed in cerebral arteries after TBI.

60-Fold Elevation of NO Levels Causes Profound Vasodilation in Cerebral Arteries After TBI

To determine the amount of excess NO responsible for attenuated myogenic constriction following TBI, we used an NO-clamp approach[11,38] and calibrated the vasodilatory response of cerebral arteries from control animals to stepwise increases in NO. Cerebral arteries (with myogenic tone) from control animals were pressurized to 70 mm Hg, and endogenous NO was negated by adding CPTIO (60 µmol/L) to scavenge existing NO and L-NNA (100 µmol/L) to inhibit

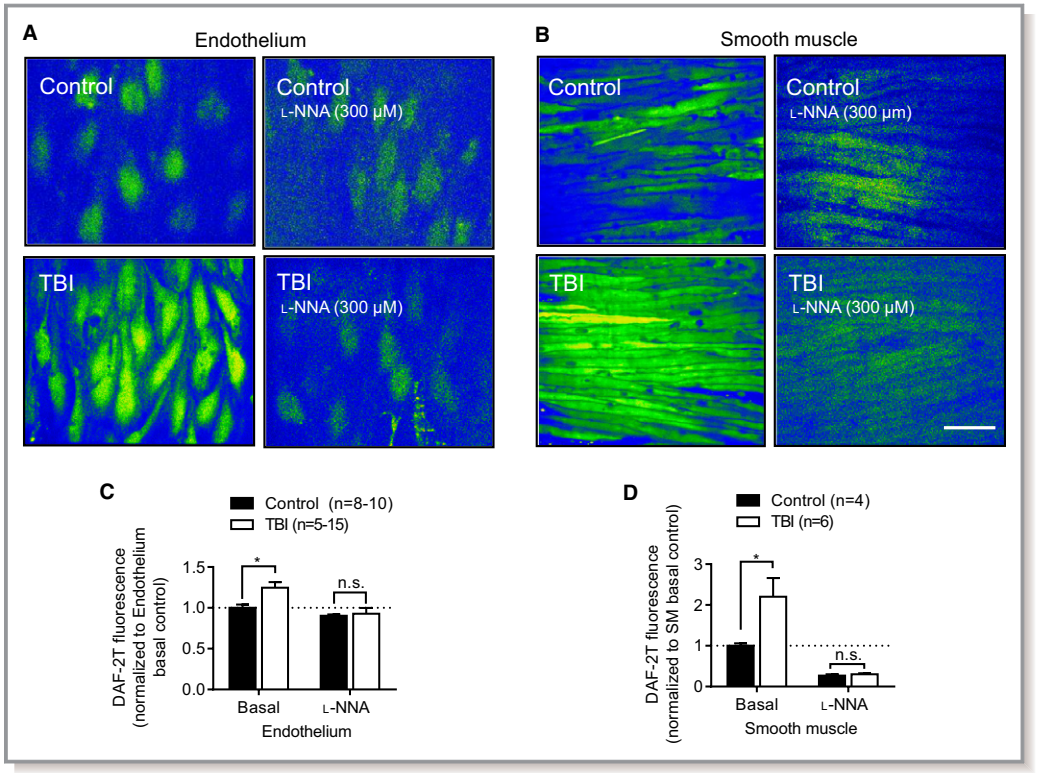

Figure 5. Nitric oxide bioavailability is increased in cerebral arteries from TBI animals compared with controls. A and B, Arteries from TBI animals exhibited a significant increase in nitric oxide levels, assessed by DAF-2T fluorescence under basal conditions in both the endothelium (left) and smooth muscle (right) that was reduced to control levels after incubation with L-NNA (300 μmol/L). C and D, Summary data of DAF-2T fluorescence with or without L-NNA normalized to basal levels in control arteries in the endothelium and smooth muscle. Wilcoxon rank-sum, **P*<0.05. Scale bar: 20 μm. DAF-2T indicates 4,5-diaminofluorescein triazole; L-NNA, Nω-nitro-L-arginine; NO, nitric oxide; TBI, traumatic brain injury.

ongoing NO synthesis. Stepwise increases in NO (0.05 to 30 nmol/L NO) revealed that the half maximal effective concentration for NO-induced dilation was 4.5 nmol/L (n=5) (Figure 9B) and that ≈30 nmol/L NO is required to simulate the loss of myogenic tone following a TBI. We found that the combination of CPTIO and L-NNA elicited a sustained constriction (18% change in diameter) that corresponded to a mean basal NO concentration of 0.4 nmol/L NO (interpolated from the concentration-response curve using clamped NO concentrations, $[NO]=10^{-9.4}$ mol/L) (Figure 9A and 9B). Using the NO-clamp approach, 30 nmol/L NO was also applied to arteries from control animals loaded with 4,5-diaminofluorescein (DAF-2). Consistent with TBI causing a 60-fold increase in cerebral artery NO, addition of 30 nmol/L NO to arteries from control animals increased DAF-2 fluorescence to comparable levels observed in arteries from TBI animals in the absence of exogenous NO (Figure 9C and 9D). Thus, 2 different observations of NO, by the fluorescent indicator and by a functional response, support the same estimate of 30 nmol/L NO in cerebral artery endothelium after TBI compared with 0.4 nmol/L in controls.

TBI-Induced Elevations of NO Dilate Cerebral Arteries via Activation of Guanylate Cyclase and Activation of SM BK Channels

We next sought to examine the downstream signaling pathway linking TBI-induced increases in NO to vasodilation. NO-mediated vasodilation classically involves activation of SM soluble guanylyl cyclase (sGC) leading to cyclic guanosine monophosphate (cGMP)-dependent protein kinase (PKG) activation.[49] Consistent with TBI evoking this canonical NO signaling pathway, a selective sGC inhibitor (ODQ, 10 μmol/L) and a cell-permeable cGMP analogue PKG inhibitor ($R_{(P)}$-8-Br-cGMPS, 1 μmol/L) restored myogenic tone to control levels in cerebral arteries isolated from TBI animals (Figure 10A through 10C). Several downstream targets have been proposed to contribute to sGC/PKG-dependent vasodilation, including SM BK channel activation.[50,51] In cerebral arteries from control animals, vasodilation evoked by spermine NONOate was reduced by BK channel blockade with paxilline (1 μmol/L) (Figure 8B), consistent with NO activation of BK channels. Furthermore, BK channel blockade with paxilline

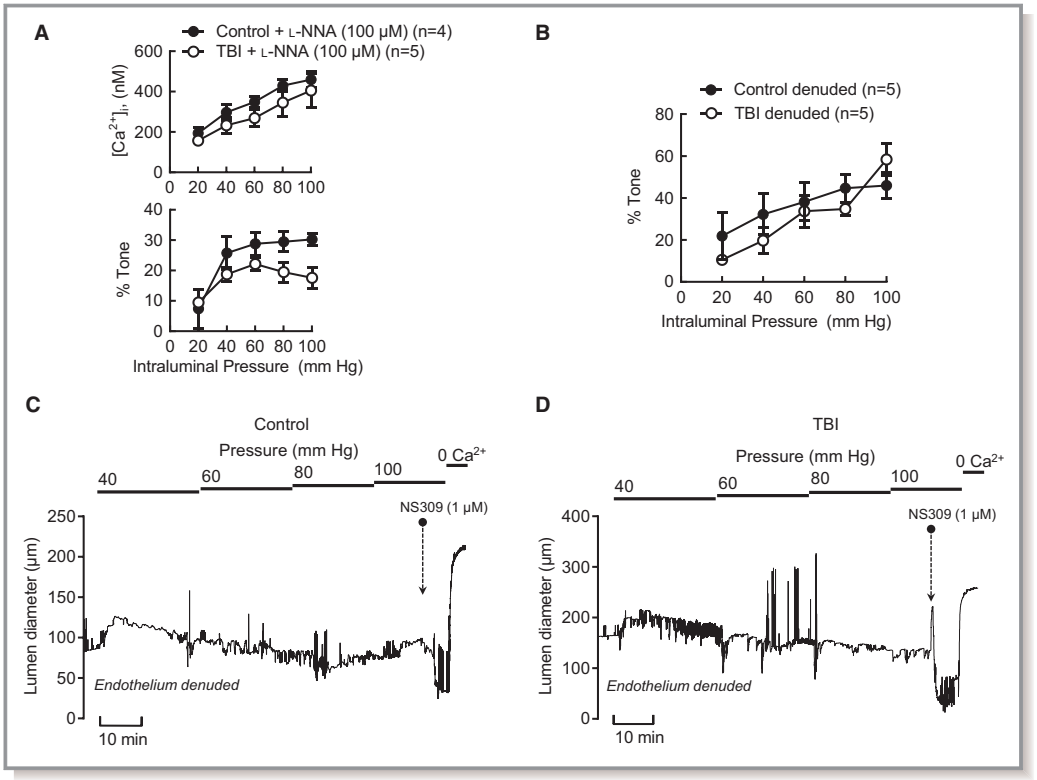

Figure 6. Differential impact of nitric oxide synthase inhibition and endothelial removal on myogenic tone in cerebral arteries from control and TBI animals. A, Summary data showing simultaneous $[Ca^{2+}]_i$ (top) and lumen diameter measurements (bottom) obtained in response to stepwise increases in intravascular pressure in arteries from control (n=4) and TBI (n=5) animals in the presence of L-NNA (100 μmol/L). B, Summary of % tone during stepwise increases in intravascular pressure obtained from endothelium denuded arteries isolated from control (n=5) and TBI (n=5) animals. C and D, Representative traces showing lumen diameter measurements obtained in response to stepwise increases in intravascular pressure in endothelium-denuded cerebral arteries from control (C) and TBI (D) animals. $[Ca^{2+}]_i$ indicates intracellular Ca^{2+} concentration; % tone, percentage of myogenic tone; L-NNA, Nω-nitro-L-arginine; TBI, traumatic brain injury.

(1 μmol/L) induced a significantly greater constriction in arteries from TBI animals compared with controls (22±6% decrease in diameter [n=7], 9±1% decrease in diameter [n=4], respectively; $P<0.05$) (Figure 10C). Collectively, these data indicate that TBI leads to an increase in endothelial NO production that acts through sGC, PKG, and BK channel activation to promote vasodilation, leading to a profound reduction in myogenic tone.

Discussion

TBI is an important global concern. This study addresses the molecular and functional changes in cerebral arteries 24 hours after brain injury in a rodent model, using intact vascular preparations with novel live-cell microscopy for NO. We report the following novel observations: (1) Pressure-dependent increases in SM Ca^{2+} and myogenic constriction are severely blunted in cerebral arteries following TBI; (2) this profound TBI-induced cerebral artery dilation is caused by a marked gain of function in endothelial NO production; (3) upregulation of the inducible isoform of NOS (iNOS), rather than the endothelial isoform (eNOS), underlies the TBI-induced increase in cerebral artery NO; (4) basal cerebral artery NO levels, estimated to be 0.4 nmol/L in control animals, increased >60-fold (to ≈30 nmol/L) after TBI; (5) the cell signaling pathway leading from iNOS-catalyzed increased endothelial NO to cerebral artery vasodilation involved activation of SM sGC, PKG, and BK channels, ultimately leading to decreased SM cytosolic Ca^{2+}. Taken together, this work suggests that upregulation of endothelial iNOS drives activation of SM BK channels to decrease SM Ca^{2+} to cause cerebral artery dilation after a TBI (Figure 11). The loss of vascular tone may result in disruption of CBF and contribute to TBI pathology. Our results suggest that selective inhibition of iNOS in endothelial cells may be a therapeutic target for medical management of TBI.

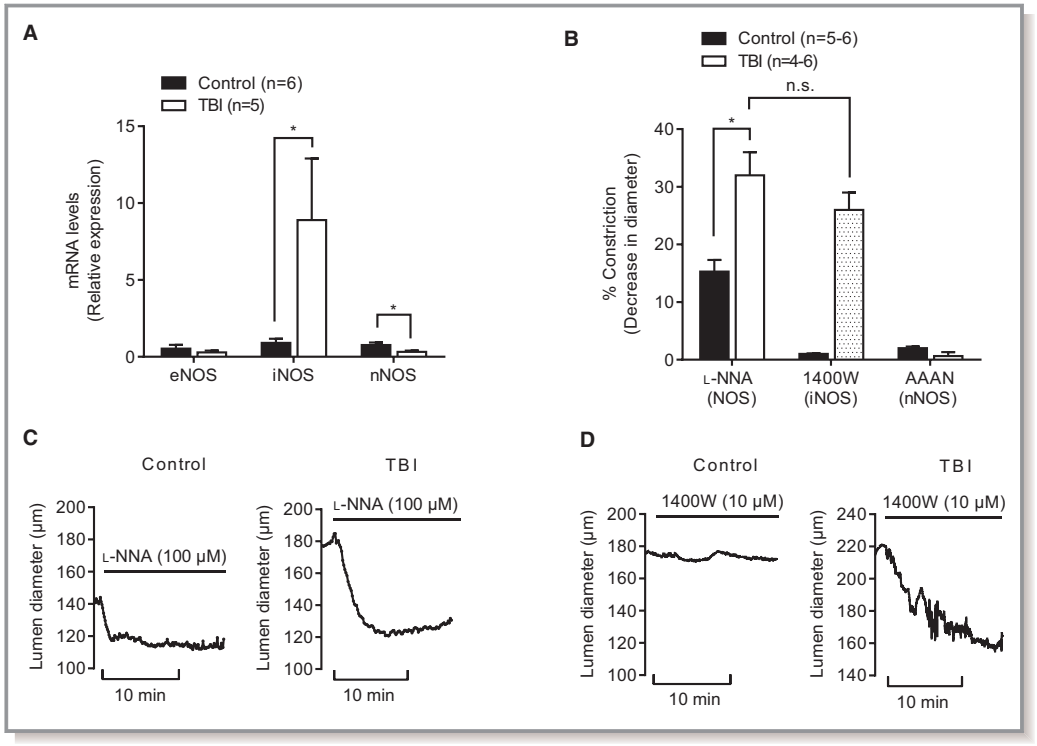

Figure 7. Relative expression of nitric oxide synthase isozymes and effect of nitric oxide synthase inhibition in cerebral arteries isolated from control and TBI animals. A, Summary data showing total mRNA levels for eNOS, iNOS, and nNOS obtained from cerebral arteries from control (n=6) and TBI (n=5) animals. B, Summary data showing percentage of constriction elicited by L-NNA (100 µmol/L), 1400W (10 µmol/L), and AAAN (1 µmol/L) in arteries pressurized to 70 mm Hg from control (n=5 to 6) and TBI (n=4 to 6) animals. Representative traces showing vasoconstriction to (C) L-NNA (100 µmol/L) and (C) 1400W (10 µmol/L) in cerebral arteries isolated from control and TBI animals. Wilcoxon rank-sum, *$P<0.05$. 1400W indicates N-([3-(aminomethyl)phenyl]methyl)-ethanimidamide, dihydrochloride; AAAN, N-[(4S)-4-amino-5-[(2-aminoethyl)amino]pentyl]-N′-nitroguanidine tris(trifluoroacetate); eNOS, endothelial isoform of nitric oxide synthase; iNOS, inducible isoform of nitric oxide synthase; L-NNA, Nω-nitro-L-arginine; nNOS, neuronal isoform of nitric oxide synthase; n.s., not significant; TBI, traumatic brain injury.

TBI Increases Cerebral Artery NO Levels ≈60-Fold

Previous studies have shown that complex changes in brain NO metabolism occur after traumatic injury,[18] but none have indexed NO in living cerebrovascular cells. Total brain NO levels are reported to increase rapidly within the first 30 minutes of injury[52,53] and then decline, possibly because of substrate depletion, leading to a period of relative NO deficiency lasting ≈6 hours.[54,55] A late-phase increase in NO then occurs that may persist for days.[56] After severe closed-head injury in humans, cerebral spinal fluid NO concentrations increase 2- to 3-fold, peaking between 30 and 42 hours, with higher levels reported in nonsurvivors.[18] Using a rat TBI animal model, total brain NO concentrations were previously shown to increase immediately following injury to 83±16 nmol/L compared with 0.5±4.0 nmol/L in the sham-injured animals[53]; however, these previous measurements were performed in intact brain with NO electrodes examining NO production in the context of direct neuronal toxicity. Furthermore, NO electrodes lack the spatial resolution to determine the vascular component of TBI-induced increases in NO. Our present study used a unique combination of live-NO imaging using the diaminofluorescein NO indicator DAF-2 DA[57] and an NO-clamp approach[11,38] that delivers set concentrations of NO to examine NO levels in isolated cerebral arteries 24 hours after fluid percussion–induced TBI in rats.

Using the combination of a long half-life NO donor and an NO scavenger, sustained concentrations of NO were mathematically modeled and accurately delivered to tissue. This NO-clamp approach was established using NO probes in vitro[38,58] and validated using an intracellular cGMP biosensor in vascular SM.[11] By calibrating the vasodilatory response of pressurized cerebral arteries in the presence of set concentrations of NO, we estimated that rat cerebral arteries have a baseline NO level of 0.4 nmol/L, achieve maximal dilation with 30 nmol/L NO, and have a half

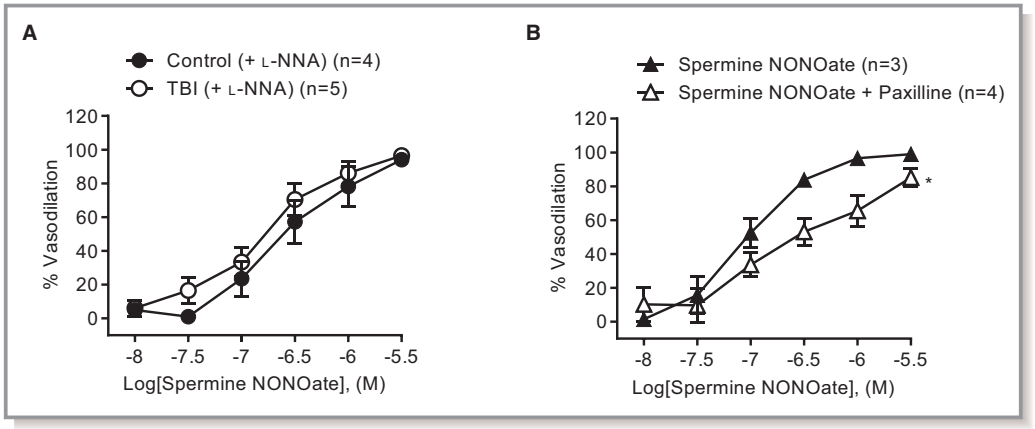

Figure 8. Sensitivity of vascular smooth muscle to exogenous nitric oxide in cerebral arteries from control and TBI animals. Summary data showing the vasodilatory response to addition of spermine NONOate in the presence of (A) L-NNA (100 μmol/L) and (B) paxilline (1 μmol/L) in arteries from control (n=3) and TBI (n=4) animals. Repeated-measures one-way ANOVA, *$P<0.05$. TBI indicates traumatic brain injury.

maximal effective concentration for vasodilation of 4.5 nmol/L (Figure 9B). This is consistent with estimates of physiological concentrations of NO in the range of 100 pmol/L to 5 nmol/L.[59]

We now provide 2 lines of evidence indicating that NO levels are increased ≈60-fold in cerebral arteries isolated from TBI model rats 24 hours after induction of injury. First, using the NO-clamp in cerebral arteries from control animals pressurized to physiological intravascular pressures, it was determined that a concentration of ≈30 nmol/L NO was required to induce the level of vasodilation observed in vessels from TBI animals. Second, using the NO indicator dye DAF-2 for live imaging of NO fluorescence in intact cerebral arteries, we observed marked elevations in both SM and endothelial cell NO after TBI (Figure 5). As an example of the use of this technique for live-cell imaging in intact blood vessels, we included a high-speed (30 frames per second) video of intracellular NO production in a cerebral artery using the DAF-2 indicator in a z-stack sweep from the lumen through endothelium and vascular SM (Video S1). Because of the much larger volume of the cells, the SM cells appear to have a higher signal, but the SM cells and endothelial cells cannot be compared directly, and quantification of NO was based on still images of confocal sections containing >14 cells per field in cross-section.

We determined that addition of 30 nmol/L NO to arteries from control animals mimicked the increased DAF-2 fluorescence observed after TBI. Consistent with the specificity of DAF-2 DA as a dynamic NO-specific indicator, we observed that the combination of the NOS inhibitor L-NNA and the NO scavenger CPTIO abolished DAF-2 fluorescence in both animal groups (Figure 5). Although prior reports have described the detection and imaging of NO with diaminofluoresceins in cultured endothelial cells,[57] we believe our study provides the first demonstration of DAF-2 to measure NO in intact endothelium and the first use of this technique to quantify TBI-induced increases of cerebrovascular NO.

Upregulation of Endothelial iNOS Underlies TBI-Induced Increases in Cerebral Artery NO and Loss of Myogenic Tone

Our data indicate that increased endothelial expression of iNOS is the major contributor to vascular NO after a TBI. Using isolated cerebral arteries, with qPCR and primer sets unique to the NOS isozymes, we observed that iNOS expression was significantly increased (Figure 7). Consistent with marked elevation in iNOS expression after TBI, the selective iNOS inhibitor 1400W constricted cerebral arteries from TBI animals but was without effect on cerebral arteries from control animals (Figure 7B). After treatment with 1400W, the level of constriction observed in arteries from TBI animals was restored to levels observed in untreated arteries from control animals. Furthermore, in arteries from TBI animals, the effect of 1400W was similar to the effect of endothelial removal (Figure 6A through 6C), suggesting TBI-induced iNOS expression occurred in endothelial cells but not in vascular SM. Previous studies have also examined iNOS expression after TBI, including a human study using tissue sections from patients who died from a TBI.[15] In postmortem tissue from human TBI victims, increased iNOS immunoreactivity was observed in neutrophils, macrophage/microglial and cerebral artery vascular SM 2 to 7 days following TBI. In addition, these authors state that endothelial cells in these vessels may also be iNOS positive.[15] Another study using

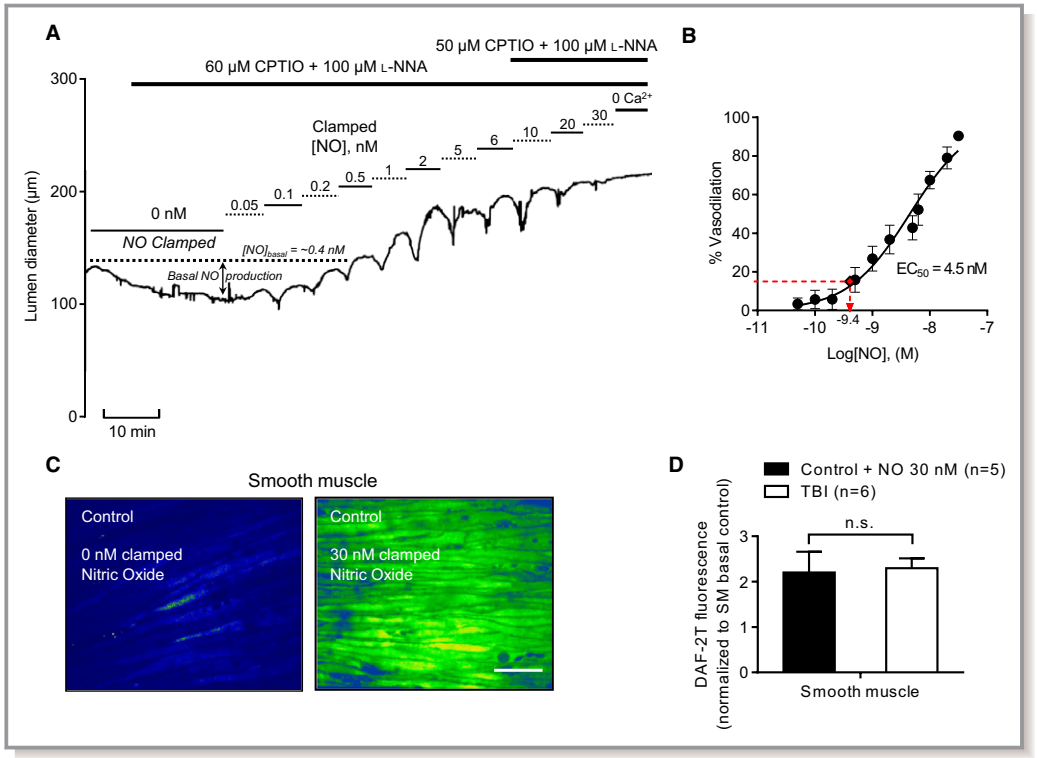

Figure 9. Vasodilatory profile of control cerebral arteries to physiological NO concentrations. A, Representative trace of a control cerebral artery pressurized to 70 mm Hg showing the vasodilatory response to stepwise increases in clamped NO concentrations. B, Summary data showing concentration and response to clamped NO, interpolated basal NO concentration and EC_{50} value (n=5). C, DAF-2T fluorescence elicited by 0 nmol/L NO and 30 nmol/L clamped NO in a control cerebral artery. D, Summary data showing DAF-2T fluorescence in basal smooth muscle from TBI (n=6) and control arteries exposed to 30 nmol/L clamped NO (n=5). DAF-2T fluorescence was normalized to basal control-level NO in SM (Wilcoxon rank-sum, ns). Scale bar: 20 μm. CPTIO indicates carboxy-2-phenyl-4,4,5,5-tetramethylimidazoline-1-oxyl-3-oxide; DAF-2T, 4,5-diaminofluorescein triazole; L-NNA, Nω-nitro-L-arginine; EC_{50}, half maximal effective concentration; NO, nitric oxide; n.s., not significant; SM, smooth muscle; TBI, traumatic brain injury.

surgically obtained tissue from TBI patients also reported increased iNOS staining in neurons, neutrophils, and macrophages.[58] Interestingly, a study relying on immunohistochemistry reported increased staining for eNOS but not for nNOS or iNOS in cerebral microvessels in rat brain slices obtained near the site of injury 1 day after fluid percussion injury.[60] We cannot exclude the possibility of a modest eNOS contribution to the increased NO levels observed in our present study, because of eNOS changes in caveolin 1 binding or phosphorylation.[61] Based on the similarity of functional responses we observed using a selective iNOS inhibitor (1400W) and a broad-spectrum NOS inhibitor (L-NNA), it appears that TBI-induced elevations in cerebral artery NO occur predominantly through increased iNOS expression. Identification of the trigger for increasing endothelial iNOS expression after TBI was outside of the scope of this work, but inflammatory responses to traumatic injury may play a role. Future studies will address the role of extracellular histones, polyphosphates, and other circulating factors that are released after trauma that might interact with the endothelium.[62]

Elevated NO Leads to Decreased SM Ca^{2+} and Loss of Myogenic Tone via Increased Activity of SM BK Channels TBI

NO plays a prominent role in the regulation of cerebral artery diameter,[12] with activation of SM soluble sGC leading to vasodilation through cGMP formation and increased activity of cGMP-dependent protein kinase (PKG) activation.[49] Several downstream sites of action have been proposed for PKG-mediated vasodilation,[49,63] including activation of large-conductance Ca^{2+}-sensitive potassium (BK) channels.[44,51] Activation of BK channels promotes membrane potential hyperpolarization and decreased Ca^{2+} influx through L-type voltage-dependent Ca^{2+} channels, leading to vasodilation.[64] We used a pharmacological approach with blockers of sGC,

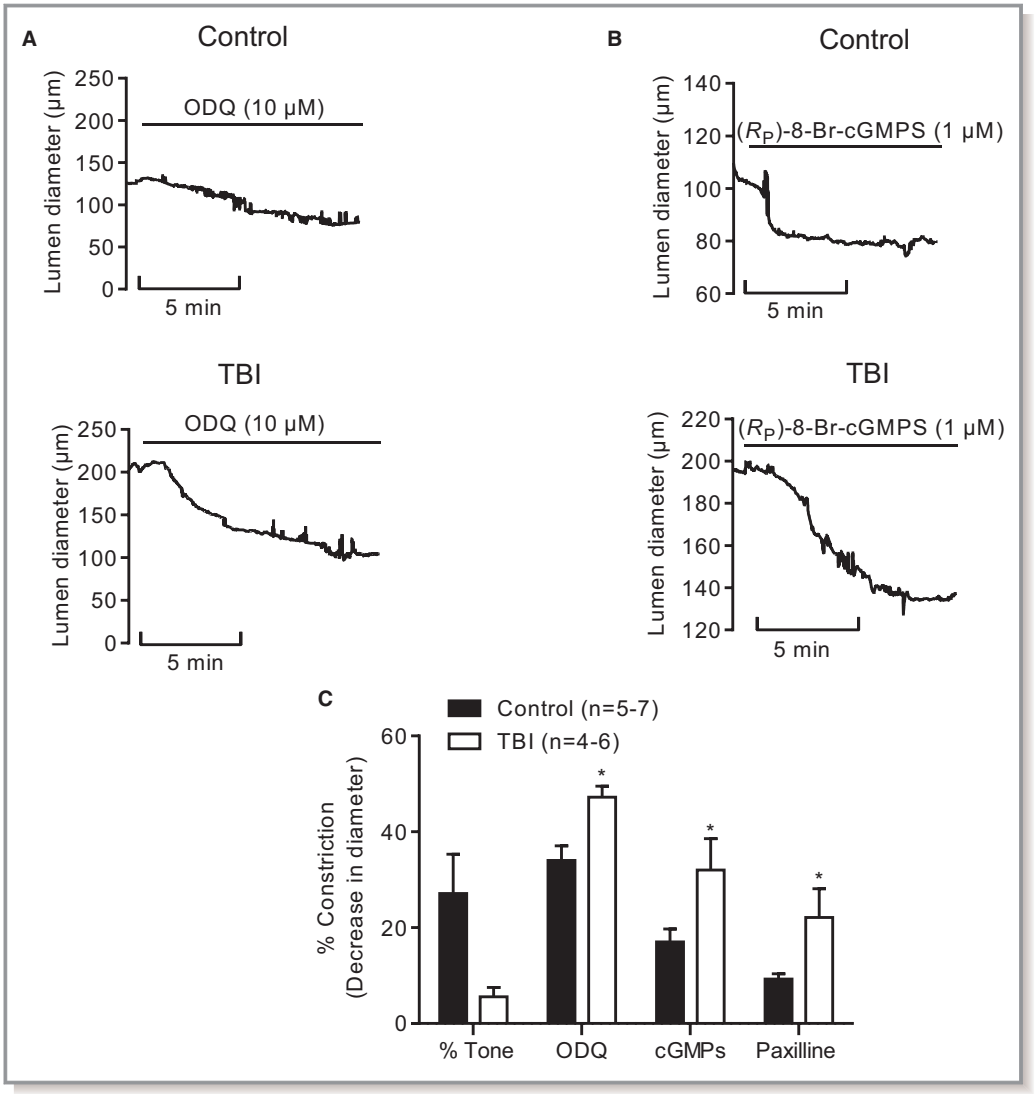

Figure 10. Effect of inhibitors of guanylyl cyclase (inhibited by ODQ), protein kinase G (inhibited by $R_{(P)}$-8-Br-cGMPS) and BK channel (inhibited by paxilline) on the diameter of cerebral arteries. Representative traces showing the effect of (A) ODQ (10 μmol/L) and (B) $R_{(P)}$-8-Br-cGMPS (1 μmol/L) on lumen diameter of arteries pressurized to 70 mm Hg from control (n=5 to 7) and TBI (n=4 to 6) animals. C, Summary data showing percentage of constriction elicited by ODQ, $R_{(P)}$-8-Br-cGMPS, and paxilline (1 μmol/L) and percentage of myogenic tone at 70 mm Hg in arteries from control and TBI animals. Wilcoxon rank-sum, $^*P<0.05$. cGMPS indicates $R_{(P)}$-8-Br-cGMPS; TBI, traumatic brain injury.

PKG, and BK channels to establish that this cell signaling pathway links TBI-induced increases in NO to vasodilation (Figure 6). Although not examined in the present study, it is likely that the observed NO-induced BK channel activity results from an increase in Ca^{2+} spark frequency.[50,65] In addition, to NO-mediated BK channel activation, it is also possible that other mechanisms[13] involving cGMP-dependent decreases in SM Ca^{2+} may contribute to TBI-induced cerebral artery dilation.[49,63] Excessive NO might also increase peroxynitrite, which might also diminish myogenic tone after TBI[4]; however, our data support a prominent role for NO-mediated, PKG-dependent activation of SM BK channels.

Clinical Implications

Complex changes in cardiovascular physiology occur after a TBI. We and others have previously shown that sympathetic nervous system activation after TBI leads to hypertension, hypercontractile cardiac function, and generation of reactive oxygen species. Blood vessels respond to changes in mechanical forces from circulating blood as shear stress and in mechanical strain as the result of heart propulsion. Among various cell signaling pathways induced by mechanical forces, a role for NO and reactive oxygen species have been implicated in several studies. Cyclic strain stimulates altered

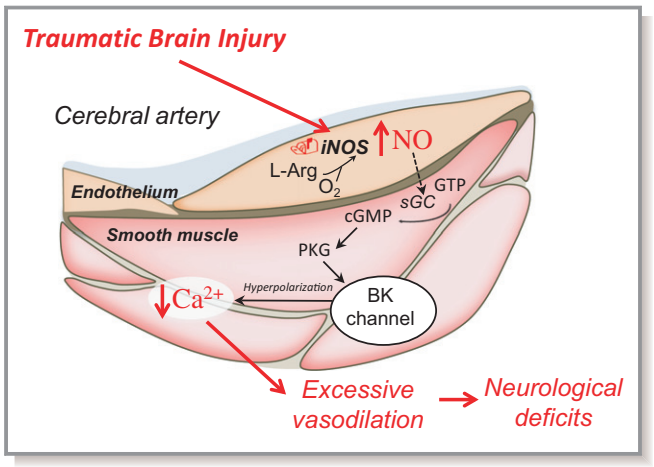

Figure 11. Overview of the mechanism by which TBI causes impaired cerebral vascular function. TBI causes an increase in iNOS expression leading to enhanced endothelial NO production, decreased smooth muscle Ca^{2+} levels, and profound cerebral artery dilation. cGMP indicates cyclic guanosine monophosphate; GTP, Guanosine-5′-triphosphate; iNOS, inducible isoform of nitric oxide synthase; L-Arg, L-arginine; NO, nitric oxide; PKG, protein kinase G; sGC, soluble guanylyl cyclase; TBI, traumatic brain injury.

gene expressions and NO/reactive oxygen species induction in cultured endothelial cells.[65,66] It is likely that sympathetic nervous system activation after a TBI induces hypertension, hyperthermia, and reactive oxygen species induction, which leads to endothelial iNOS upregulation and vasodilation of the cerebral arteries (Figure 11).

Our observations suggest several additional lines of research that might provide insight into the vascular effects of TBI. Because the regulation of vascular tone is mechanically different between small vessels and larger vessels, it would be of interest to further elucidate the differences between small vessels such as mesenteric resistance arteries and larger vessels such as aorta. In addition, we cannot exclude the contribution of adventitial cells or circulating inflammatory cells, which might bind to endothelium after trauma.

We have not ruled out possible contributions by alterations in cyclooxygenase metabolites, the prostanoid synthesizing enzymes constitutively expressed in the brain, which also could contribute to responses to TBI. Reductions in hypometabolism may also contribute to changes in CBF after brain trauma. Additional studies of longitudinal effects over a longer time course after TBI, in women, or using older animals would also be of interest.

Presently, it is unclear if the observed 60-fold increase in endothelial NO levels is a protective, adaptive response or a contributor to deleterious consequences after TBI. Studies have examined both NO administration and NO inhibition after TBI, with conflicting results.[27,53,68] A study with iNOS null-mice, for example, suggested that iNOS provides modest improvement in long-term behavioral outcomes after TBI (20 days) but did not include any data about cerebrovascular function, neurovascular coupling, CBF, or edema. NO concentration influences basal tone, and both excess and deficiency of NO may contribute to brain pathologies after TBI. NO overproduction by neuronal iNOS, for example, can yield micromolar concentrations of NO that mediate nitrosylation processes and neurotoxicity. Conversely, NO underproduction, due to vascular eNOS knockout or phosphorylation, has been implicated in impairment of cerebral perfusion in cerebral ischemia models.[27,61] Thus, an increase of vascular NO levels in the range of 30 nmol/L might be neuroprotective by increasing perfusion, protecting the concussed brain from ischemia and breakdown of the blood–brain barrier. In contrast, excessive vasodilation of cerebral arteries in the days after a TBI could also contribute to cerebral edema, diffuse hemorrhage, and intracranial hypertension. Studies of NO inhibition in vivo have provided conflicting results. During the initial peak of NO, the administration of L-NAME did not improve outcome or cause resolution of neurological deficits; however, inhibition of iNOS in the late phase after TBI was shown to be neuroprotective in experimental models of TBI.[28,30,69] Furthermore, NO inhalation to increase NO levels was reported to benefit mice after TBI.[22] Future work is needed to determine whether targeted iNOS inhibitors or other modulators of this pathway might provide therapeutic benefit after TBI.

Conclusions

TBI causes profound cerebral artery vasodilation resulting from a 60-fold elevation of NO production via upregulation of endothelial iNOS. In addition, TBI-mediated increased endothelial NO production acts through sGC, PKG, and SM BK channel activation to cause vasodilation and ablation of myogenic tone. This loss of myogenic tone, a major contributor to cerebral autoregulation, may represent a significant aspect of TBI pathology.

Appendix

Supplementary Video: Intracellular NO, indexed by 4,5-dianimofluorescein (DAF-2) fluorescence, in the endothelium and smooth muscle of a live cerebral blood vessel.

The video shows the wall of a cerebral blood vessel in a field of view of ≈113×136 μm, using high-speed (30 to 35 frames per second) image acquisition of intracellular NO-indicator fluorescence in a z-stack sweep from the luminal surface of the endothelial cells through vascular smooth muscle.

Acknowledgments

Dr Adrian Bonev assisted with microscopy and analysis; Drs Wolfgang Dostmann and Kara Held advised on clamped NO methodology; Dr Natalia Gokina provided help with smooth muscle Ca^{2+} measurements; Ivette Nunez and Sheila Russell provided valuable technical support.

Sources of Funding

American Heart Association fellowships to Drs Villalba, Longden (13POST14820015, 12POST12090001); and additional funding from the Totman Medical Research Trust, Fondation Leducq, Peter A. Martin Brain Aneurysm Research Fund, and National Institutes of Health (P20-RR-16435, P01-HL-095488, UM1-HL-120877-01, R01-HL-044455, R01-HL-098243, R37-DK-053832, P30-RR-032135-02, P30-GM-103498-02, K08-GM-098795-01, K99-HL-121484-01, R01-HL-121706-01).

Disclosures

None.

References

1. Marin JR, Weaver MD, Yealy DM, Mannix RC. Trends in visits for traumatic brain injury to emergency departments in the United States. *JAMA*. 2014;311:1917–1919.
2. Golding EM, Contant CF, Robertson CS, Bryan RM. Temporal effect of severe controlled cortical impact injury in the rat on the myogenic response of the middle cerebral artery. *J Neurotrauma*. 1998;15:973–984.
3. Mathew BP, DeWitt DS, Bryan RM, Bukoski RD, Prough DS. Traumatic brain injury reduces myogenic responses in pressurized rodent middle cerebral arteries. *J Neurotrauma*. 1999;16:1177–1186.
4. Yu GX, Mueller M, Hawkins BE, Mathew BP, Parsley MA, Vergara LA, Hellmich HL, Prough DS, Dewitt DS. Traumatic brain injury in vivo and in vitro contributes to cerebral vascular dysfunction through impaired gap junction communication between vascular smooth muscle cells. *J Neurotrauma*. 2014;31:739–748.
5. Bryan RM Jr, Cherian L, Robertson C. Regional cerebral blood flow after controlled cortical impact injury in rats. *Anesth Analg*. 1995;80:687–695.
6. Richards HK, Simac S, Piechnik S, Pickard JD. Uncoupling of cerebral blood flow and metabolism after cerebral contusion in the rat. *J Cereb Blood Flow Metab*. 2001;21:779–781.
7. Foley LM, Iqbal O'Meara AM, Wisniewski SR, Hitchens TK, Melick JA, Ho C, Jenkins LW, Kochanek PM. MRI assessment of cerebral blood flow after experimental traumatic brain injury combined with hemorrhagic shock in mice. *J Cereb Blood Flow Metab*. 2013;33:129–136.
8. Hendrich KS, Kochanek PM, Williams DS, Schiding JK, Marion DW, Ho C. Early perfusion after controlled cortical impact in rats: quantification by arterial spin-labeled MRI and the influence of spin-lattice relaxation time heterogeneity. *Magn Reson Med*. 1999;42:673–681.
9. Faraci FM, Heistad DD. Regulation of the cerebral circulation: role of endothelium and potassium channels. *Physiol Rev*. 1998;78:53–97.
10. Faraci FM, Brian JE Jr. Nitric oxide and the cerebral circulation. *Stroke*. 1994;25:692–703.
11. Held KF, Dostmann WR. Sub-nanomolar sensitivity of nitric oxide mediated regulation of cGMP and vasomotor reactivity in vascular smooth muscle. *Front Pharmacol*. 2012;3:130.
12. Pelligrino DA, Koenig HM, Albrecht RF. Nitric oxide synthesis and regional cerebral blood flow responses to hypercapnia and hypoxia in the rat. *J Cereb Blood Flow Metab*. 1993;13:80–87.
13. Nathan C, Xie QW. Nitric oxide synthases: roles, tolls, and controls. *Cell*. 1994;78:915–918.
14. Gahm C, Holmin S, Mathiesen T. Nitric oxide synthase expression after human brain contusion. *Neurosurgery*. 2002;50:1319–1326.
15. Orihara Y, Ikematsu K, Tsuda R, Nakasono I. Induction of nitric oxide synthase by traumatic brain injury. *Forensic Sci Int*. 2001;123:142–149.
16. Gahm C, Holmin S, Mathiesen T. Temporal profiles and cellular sources of three nitric oxide synthase isoforms in the brain after experimental contusion. *Neurosurgery*. 2000;46:169–177.
17. Rafols D, Steiner J, Rafols JA, Petrov T. Intracellular coexpression of endothelin-1 and inducible nitric oxide synthase underlies hypoperfusion after traumatic brain injury in the rat. *Neurosci Lett*. 2004;362:154–157.
18. Cherian L, Hlatky R, Robertson CS. Nitric oxide in traumatic brain injury. *Brain Pathol*. 2004;14:195–201.
19. Rodriguez-Baeza A, Reina-de la Torre F, Poca A, Marti M, Garnacho A. Morphological features in human cortical brain microvessels after head injury: a three-dimensional and immunocytochemical study. *Anat Rec A Discov Mol Cell Evol Biol*. 2003;273:583–593.
20. Golding EM, Steenberg ML, Cherian L, Marrelli SP, Robertson CS, Bryan RM. Endothelial-mediated dilations following severe controlled cortical impact injury in the rat middle cerebral artery. *J Neurotrauma*. 1998;15:635–644.
21. Golding EM, You J, Robertson CS, Bryan RM. Potentiated endothelium-derived hyperpolarizing factor-mediated dilations in cerebral arteries following mild head injury. *J Neurotrauma*. 2001;18:691–697.
22. Terpolilli NA, Kim SW, Thal SC, Kuebler WM, Plesnila N. Inhaled nitric oxide reduces secondary brain damage after traumatic brain injury in mice. *J Cereb Blood Flow Metab*. 2013;33:311–318.
23. Golding EM, Robertson CS, Fitch JCK, Goodman JC, Bryan RM. Segmental vascular resistance after mild controlled cortical impact injury in the rat. *J Cereb Blood Flow Metab*. 2003;23:210–218.
24. Ahn M-J, Sherwood ER, Prough DS, Lin CY, DeWitt DS. The effects of traumatic brain injury on cerebral blood flow and brain tissue nitric oxide levels and cytokine expression. *J Neurotrauma*. 2004;21:1431–1442.
25. Wei L, Zhang Y, Yang C, Wang Q, Zhuang Z, Sun Z. Neuroprotective effects of ebselen in traumatic brain injury model: involvement of nitric oxide and p38 mitogen-activated protein kinase signalling pathway. *Clin Exp Pharmacol Physiol*. 2014;41:134–138.
26. Petrov T, Page AB, Owen CR, Rafols JA. Expression of the inducible nitric oxide synthase in distinct cellular types after traumatic brain injury: an in situ hybridization and immunocytochemical study. *Acta Neuropathol*. 2000;100:196–204.
27. Huang Z, Huang PL, Ma J, Meng W, Ayata C, Fishman MC, Moskowitz MA. Enlarged infarcts in endothelial nitric oxide synthase knockout mice are attenuated by nitro-L-arginine. *J Cereb Blood Flow Metab*. 1996;16:981–987.
28. Lu J, Moochhala S, Shirhan M, Ng KC, Teo AL, Tan MH, Moore XL, Wong MC, Ling EA. Neuroprotection by aminoguanidine after lateral fluid-percussive brain injury in rats: a combined magnetic resonance imaging, histopathologic and functional study. *Neuropharmacology*. 2003;44:253–263.
29. Wada K, Chatzipanteli K, Kraydieh S, Busto R, Dietrich WD. Inducible nitric oxide synthase expression after traumatic brain injury and neuroprotection with aminoguanidine treatment in rats. *Neurosurgery*. 1998;43:1427–1436.
30. Jafarian-Tehrani M, Louin G, Royo NC, Besson VC, Bohme GA, Plotkine M, Marchand-Verrecchia C. 1400w, a potent selective inducible NOS inhibitor, improves histopathological outcome following traumatic brain injury in rats. *Nitric Oxide*. 2005;12:61–69.
31. Larson BE, Stockwell DW, Boas S, Andrews T, Wellman GC, Lockette W, Freeman K. Cardiac reactive oxygen species after traumatic brain injury. *J Surg Res*. 2012;173:e73–e81.
32. Kabadi SV, Hilton GD, Stoica BA, Zapple DN, Faden AI. Fluid-percussion-induced traumatic brain injury model in rats. *Nat Protoc*. 2010;5:1552–1563.
33. Knot HJ, Nelson MT. Regulation of arterial diameter and wall [Ca^{2+}] in cerebral arteries of rat by membrane potential and intravascular pressure. *J Physiol*. 1998;508(Pt 1):199–209.
34. Nystoriak MA, O'Connor KP, Sonkusare SK, Brayden JE, Nelson MT, Wellman GC. Fundamental increase in pressure-dependent constriction of brain parenchymal arterioles from subarachnoid hemorrhage model rats due to membrane depolarization. *Am J Physiol Heart Circ Physiol*. 2011;300:803–812.
35. Dacey RG, Duling BR. A study of rat intracerebral arterioles: methods, morphology, and reactivity. *Am J Physiol*. 1982;243:H598–H606.
36. Hannah RM, Dunn KM, Bonev AD, Nelson MT. Endothelial SK(Ca) and IK(Ca) channels regulate brain parenchymal arteriolar diameter and cortical cerebral blood flow. *J Cereb Blood Flow Metab*. 2011;31:1175–1186.

37. Grynkiewicz G, Poenie M, Tsien RY. A new generation of Ca^{2+} indicators with greatly improved fluorescence properties. *J Biol Chem*. 1985;260:3440–3450.
38. Griffiths C, Wykes V, Bellamy TC, Garthwaite J. A new and simple method for delivering clamped nitric oxide concentrations in the physiological range: application to activation of guanylyl cyclase-coupled nitric oxide receptors. *Mol Pharmacol*. 2003;64:1349–1356.
39. Kojima H, Sakurai K, Kikuchi K, Kawahara S, Kirino Y, Nagoshi H, Hirata Y, Nagano T. Development of a fluorescent indicator for nitric oxide based on the fluorescein chromophore. *Chem Pharm Bull (Tokyo)*. 1998;46:373–375.
40. Sonkusare SK, Bonev AD, Ledoux J, Liedtke W, Kotlikoff MI, Heppner TJ, Hill-Eubanks DC, Nelson MT. Elementary Ca^{2+} signals through endothelial TRPV4 channels regulate vascular function. *Science (New York, NY)*. 2012;336:597–601.
41. Ledoux J, Taylor MS, Bonev AD, Hannah RM, Solodushko V, Shui B, Tallini Y, Kotlikoff MI, Nelson MT. Functional architecture of inositol 1,4,5-trisphosphate signaling in restricted spaces of myoendothelial projections. *Proc Natl Acad Sci USA*. 2008;105:9627–9632.
42. Longden TA, Dabertrand F, Hill-Eubanks DC, Hammack SE, Nelson MT. Stress-induced glucocorticoid signaling remodels neurovascular coupling through impairment of cerebrovascular inwardly rectifying K^+ channel function. *Proc Natl Acad Sci USA*. 2014;111:7462–7467.
43. Livak KJ, Schmittgen TD. Analysis of relative gene expression data using real-time quantitative PCR and the 2(-Delta Delta C(T)) method. *Methods*. 2001;25:402–408.
44. Wellman GC, Bonev AD, Nelson MT, Brayden JE. Gender differences in coronary artery diameter involve estrogen, nitric oxide, and Ca(2+)-dependent K^+ channels. *Circ Res*. 1996;79:1024–1030.
45. Garvey EP, Oplinger JA, Furfine ES, Kiff RJ, Laszlo F, Whittle BJ, Knowles RG. 1400w is a slow, tight binding, and highly selective inhibitor of inducible nitric-oxide synthase in vitro and in vivo. *J Biol Chem*. 1997;272:4959–4963.
46. Zhang P, Xu X, Hu X, van Deel ED, Zhu G, Chen Y. Inducible nitric oxide synthase deficiency protects the heart from systolic overload-induced ventricular hypertrophy and congestive heart failure. *Circ Res*. 2007;100:1089–1098.
47. Takimoto Y, Aoyama T, Tanaka K, Keyamura R, Yui Y, Sasayama S. Augmented expression of neuronal nitric oxide synthase in the atria parasympathetically decreases heart rate during acute myocardial infarction in rats. *Circulation*. 2002;105:490–496.
48. Hah JM, Roman LJ, Martasek P, Silverman RB. Reduced amide bond peptidomimetics. (4S)-N-(4-amino-5-[aminoakyl]aminopentyl)-N′-nitroguanidines, potent and highly selective inhibitors of neuronal nitric oxide synthase. *J Med Chem*. 2001;44:2667–2670.
49. Lincoln TM, Dey N, Sellak H. Invited review: cGMP-dependent protein kinase signaling mechanisms in smooth muscle: from the regulation of tone to gene expression. *J Appl Physiol (1985)*. 2001;91:1421–1430.
50. Porter VA, Bonev AD, Knot HJ, Heppner TJ, Stevenson AS, Kleppisch T, Lederer WJ, Nelson MT. Frequency modulation of Ca^{2+} sparks is involved in regulation of arterial diameter by cyclic nucleotides. *Am J Physiol*. 1998;274:C1346–C1355.
51. Robertson BE, Schubert R, Hescheler J, Nelson MT. cGMP-dependent protein kinase activates Ca-activated K channels in cerebral artery smooth muscle cells. *Am J Physiol*. 1993;265:C299–C303.
52. Muir JK, Boerschel M, Ellis EF. Continuous monitoring of posttraumatic cerebral blood flow using laser-Doppler flowmetry. *J Neurotrauma*. 1992;9:355–362.
53. Cherian L, Goodman JC, Robertson CS. Brain nitric oxide changes after controlled cortical impact injury in rats. *J Neurophysiol*. 2000;83:2171–2178.
54. Yuan XQ, Wade CE, Prough DS, DeWitt DS. Traumatic brain injury creates biphasic systemic hemodynamic and organ blood flow responses in rats. *J Neurotrauma*. 1990;7:141–153.
55. Yamakami I, McIntosh TK. Effects of traumatic brain injury on regional cerebral blood flow in rats as measured with radiolabeled microspheres. *J Cereb Blood Flow Metab*. 1989;9:117–124.
56. Clark RS, Kochanek PM, Obrist WD, Wong HR, Billiar TR, Wisniewski SR, Marion DW. Cerebrospinal fluid and plasma nitrite and nitrate concentrations after head injury in humans. *Crit Care Med*. 1996;24:1243–1251.
57. Yi FX, Zhang AY, Campbell WB, Zou AP, Van Breemen C, Li PL. Simultaneous in situ monitoring of intracellular Ca^{2+} and NO in endothelium of coronary arteries. *Am J Physiol Heart Circ Physiol*. 2002;283:H2725–H2732.
58. Bellamy TC, Griffiths C, Garthwaite J. Differential sensitivity of guanylyl cyclase and mitochondrial respiration to nitric oxide measured using clamped concentrations. *J Biol Chem*. 2002;277:31801–31807.
59. Hall CN, Garthwaite J. What is the real physiological no concentration in vivo? *Nitric Oxide*. 2009;21:92–103.
60. Cobbs CS, Fenoy A, Bredt DS, Noble LJ. Expression of nitric oxide synthase in the cerebral microvasculature after traumatic brain injury in the rat. *Brain Res*. 1997;751:336–338.
61. Li Q, Atochin D, Kashiwagi S, Earle J, Wang A, Mandeville E, Hayakawa K, d'Uscio LV, Lo EH, Katusic Z, Sessa W, Huang PL. Deficient eNOS phosphorylation is a mechanism for diabetic vascular dysfunction contributing to increased stroke size. *Stroke*. 2013;44:3183–3188.
62. Abrams ST, Zhang N, Manson J, Liu T, Dart C, Baluwa F, Wang SS, Brohi K, Kipar A, Yu W, Wang G, Toh CH. Circulating histones are mediators of trauma-associated lung injury. *Am J Respir Crit Care Med*. 2013;187:160–169.
63. Hofmann F, Ammendola A, Schlossmann J. Rising behind NO: cGMP-dependent protein kinases. *J Cell Sci*. 2000;113(Pt 10):1671–1676.
64. Nelson MT, Huang Y, Brayden JE, Hescheler J, Standen NB. Arterial dilations in response to calcitonin gene-related peptide involve activation of K^+ channels. *Nature*. 1990;344:770–773.
65. Wellman GC, Nelson MT. Signaling between SR and plasmalemma in smooth muscle: sparks and the activation of Ca^{2+}-sensitive ion channels. *Cell Calcium*. 2003;34:211–229.
66. Hishikawa K, Luscher TF. Pulsatile stretch stimulates superoxide production in human aortic endothelial cells. *Circulation*. 1997;96:3610–3616.
67. Cheng JJ, Wung BS, Chao YJ, Hsieh HJ, Wang DL. Cyclic strain induces redox changes in endothelial cells. *Chin J Physiol*. 1999;42:103–111.
68. Sinz EH, Kochanek PM, Dixon CE, Clark RS, Carcillo JA, Schiding JK, Chen M, Wisniewski SR, Carlos TM, Williams D, DeKosky ST, Watkins SC, Marion DW, Billiar TR. Inducible nitric oxide synthase is an endogenous neuroprotectant after traumatic brain injury in rats and mice. *J Clin Invest*. 1999;104:647–656.
69. Louin G, Marchand-Verrecchia C, Palmier B, Plotkine M, Jafarian-Tehrani M. Selective inhibition of inducible nitric oxide synthase reduces neurological deficit but not cerebral edema following traumatic brain injury. *Neuropharmacology*. 2006;50:182–190.